COMPARISON OF THE OXIDE STRUCTURE FORMED ON 9CrODS STEEL AND NF616 IN SUPERCRITICAL WATER

J. Bischoff[1], A.T. Motta[1]
[1]*Department of Mechanical and Nuclear Engineering, the Pennsylvania State University, 227 Reber Building, University Park, PA, 16802.*

X. Ren[2], T.R. Allen[2]
[2] *Department of Engineering Physics, University of Wisconsin-Madison, 1500 Engineering Drive, Madison, WI 53706, USA.*

The microstructure of the oxide layers formed on both a 9CrODS alloy and NF616 exposed to 600ºC supercritical water was characterized using microbeam synchrotron radiation diffraction and fluorescence. This analysis was complemented by SEM observations. Both alloys contain about 9 wt% of chromium and exhibited a three layer structure with an outer layer containing Fe_3O_4, an inner layer containing a mixture of Fe_3O_4 and $FeCr_2O_4$, and an internal oxidation layer containing a mixture of oxide precipitates and metal grains. Nevertheless, the 9CrODS alloy studied had much thinner oxide layer thicknesses when corroded in the same environment, suggesting improved corrosion resistance due to the influence of the ODS particles. Additionally, one of the NF616 samples was coated with an yttrium layer on its surface prior to oxidation, which enabled the study of such a layer on the corrosion resistance of the alloy in comparison to the presence of ODS particles in the matrix.

I. INTRODUCTION

The Supercritical Water Reactor is one of the six Generation IV nuclear power plant designs and was envisioned for its high thermal efficiency and simplified core [1]. This reactor is designed to function at high outlet temperature (between 500ºC and 600ºC), which requires cladding and structural materials with good corrosion resistance. Because of their resistance to void swelling and to stress corrosion cracking, ferritic-martensitic steels, such as NF616, are candidates for the supercritical water reactor. The recently developed oxide dispersion strengthened (ODS) alloys exhibit enhanced corrosion resistance and other high temperature properties compared to conventional ferritic steels, and are therefore also envisioned for such an application [2, 3]. ODS alloys contain a fine dispersion of yttrium rich oxide nano-particles in the matrix.

The enhanced oxidation behavior of ODS steels has been suggested to be due to the Reactive Element Effect (REE) caused by the presence of yttrium rich nano-particles in the matrix [4]. The presence of yttrium in the matrix is believed to have several beneficial effects such as its segregation to the grain boundaries, which slows down the diffusion processes [2, 4]. Additionally, the presence of a small amount of yttrium appears to diminish the minimum chromium content needed to form Cr_2O_3 which plays an active role in the corrosion resistance of a material [4]. The beneficial effect of yttrium can also be partially obtained by implanting an yttrium layer at the surface of the metal prior to oxidation. The NF616 sample exposed for 4 weeks was coated with such a layer prior to oxidation so we will be able to see how it affects the corrosion behavior.

This study compares the microstructure of the oxide layers formed on NF616 and 9CrODS alloy, both of which contain about 9 wt% chromium. The 9CrODS alloy was developed by the Japan Atomic Energy Agency for application in sodium-cooled fast reactors [5, 6]. The microstructure of the oxide layer formed on the 9CrODS alloy exposed to supercritical water was analyzed in a previous article, the main points of which will be reviewed here for comparison with NF616 [7]. Both alloys have been corroded in 600ºC supercritical water for three exposure times: 2, 4 and 6 weeks. The main technique used to characterize the oxide layers was microbeam synchrotron radiation diffraction and fluorescence, and was complemented by scanning electron microscopy (SEM).

II. EXPERIMENTAL PROCEDURES

As shown in Table 1, both NF616 and the 9CrODS alloy contain about 9 wt% chromium. The 9CrODS alloy is a ferritic steel containing mechanically alloyed yttrium-rich oxide nano-particles in the matrix [5, 6]. NF616 on the other hand has a duplex ferritic and martensitic lath structure. Although the metal microstructure is slightly different in both alloys, it is the chromium content that mainly determines the corrosion resistance of the alloy [8].

The main characterization technique used in the study is microbeam synchrotron radiation diffraction and fluorescence. These experiments were performed at the 2-ID-D beamline of the APS facility at Argonne National Laboratory. In this experiment, the beam is focused to 0.2 μm and is scanned step by step across the oxide layer. At

each step fluorescence (elemental information) and diffraction data (phase information) is acquired simultaneously. Thus we obtain phase and elemental distribution as a function of distance in the oxide. The sample preparation and setup for the microbeam synchrotron radiation experiment have already been described in a previous article [7]. The diffraction peaks are shown for a beam energy of 9.5 keV.

The corrosion experiments were performed at the supercritical water loop at the University of Wisconsin using a pressure of 25 MPa, a temperature of 600ºC, and an oxygen content of 25 ppb [9, 10]. The exposure times for both samples were 2, 4 and 6 weeks.

III. RESULTS

Figure 1 shows SEM images and corresponding synchrotron fluorescence scans of the oxide layers formed on 9CrODS at 2, 4 and 6 weeks [7]. The SEM images show a three-layer structure. As shown by the analysis of the diffraction data, the outer layer contains only Fe_3O_4, the inner layer is a mixture of $FeCr_2O_4$ and Fe_3O_4, and the internal oxidation layer (also called diffusion layer) is a mixture of metal grains and oxide precipitates, which are essentially $FeCr_2O_4$ and Cr_2O_3. Additionally, Cr_2O_3 was observed at the inner-internal oxidation layer interface in the 2 and 4-week samples, and a Cr_2O_3 film appeared in the 4 and 6-week samples at the internal oxidation layer-metal interface. In all cases, the outer-inner layer interface is very distinct and is thought to be the original water-metal interface [3]. This interface is used as the zero point in the fluorescence and diffraction plots.

TABLE 1: Elemental composition of the 9CrODS alloy and NF616 in wt% with balanced iron content.

Alloy	C	Al	Si	P	S	Ti	V	Cr	Mn	Ni	Nb	Mo	W	Others
9CrODS	0.14	-	0.048	<0.005	0.003	0.21	-	8.6	0.05	0.06	-	-	2	Y: 0.28 O: 0.14
NF616	.109	.005	0.102	0.012	.003	-	.194	8.82	0.45	0.174	.064	0.468	1.87	O: 0.0042

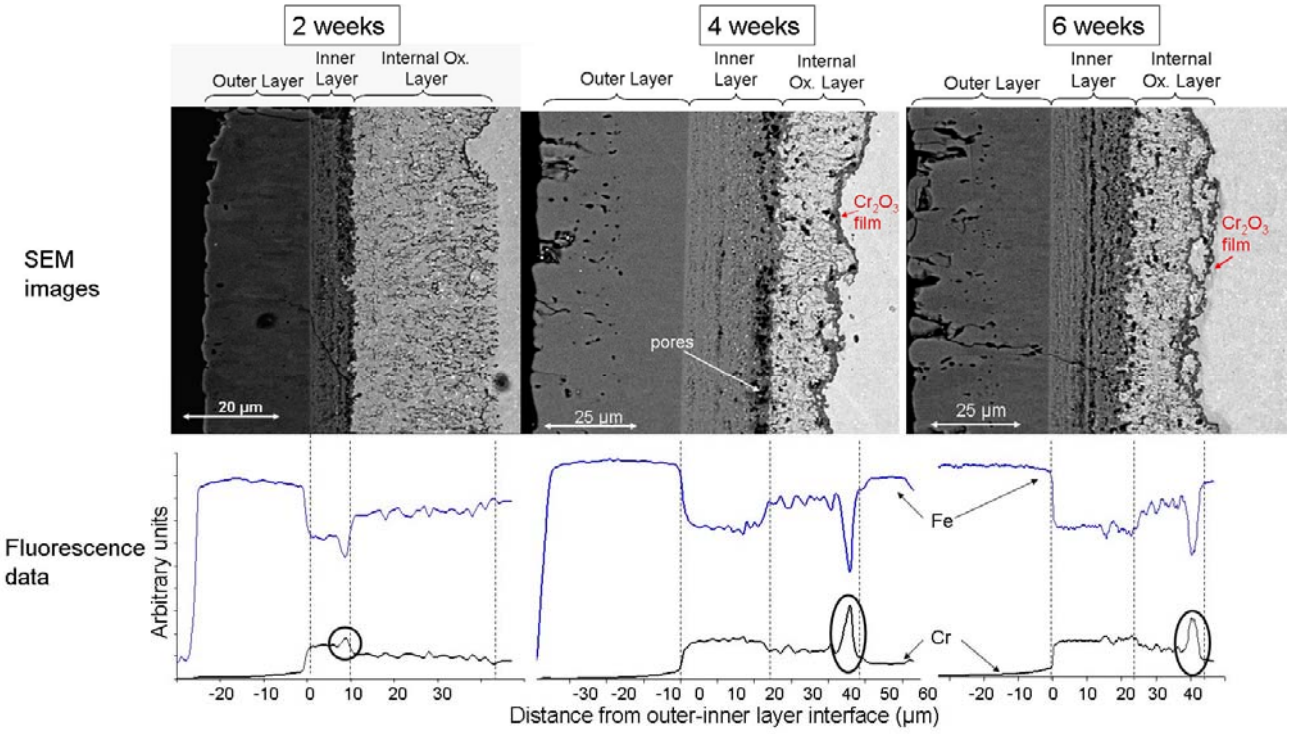

Figure 1: SEM images and fluorescence data showing the evolution with time of the microstructure of the oxide layer formed on 9CrODS alloy exposed to 600ºC supercritical water.

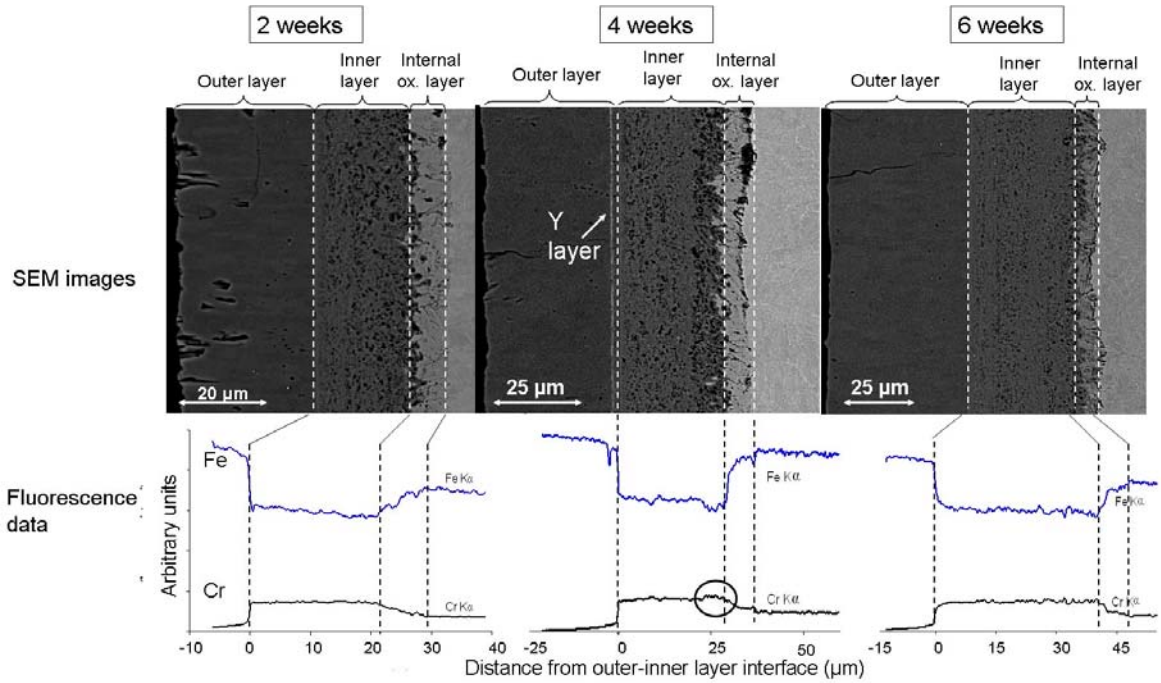

Figure 2: SEM images and fluorescence data showing the evolution with time of the microstructure of the oxide layer formed on NF616 alloy exposed to 600ºC supercritical water.

The fluorescence scans show that the inner layer is enriched in chromium compared to the metal, likely because iron migrates outwards to form the outer layer, leaving a chromium enriched region behind. A more localized enrichment of chromium (circled) is observed at the inner-internal oxidation layer interface for the 9CrODS 2-week sample, where Cr_2O_3 is also observed. In the 4 and 6-week samples this localized chromium enrichment has shifted to the internal oxidation layer-metal interface. Between 2 and 4 weeks, a Cr_2O_3 film appeared at the internal oxidation layer-metal interface, which can be observed in the SEM images. The internal oxidation layer-metal interface is remarkably straight in the 2-week sample but becomes jagged in the 4 and 6-week samples, likely as a result of the appearance of the Cr_2O_3 film.

Additionally, for both the 2 and 4-week samples, the interface between the inner and internal oxidation layers is relatively straight and is outlined by a line of pores. In the 6-week sample on the other hand, this interface is jagged and the pores are more spread out. This difference has been attributed to the presence of Cr_2O_3 at the interface in the 2 and 4-week samples and its absence in the 6-week sample [11]. Finally, the SEM images show that the outer layer becomes more porous with longer exposure times.

The SEM images and fluorescence data in Figure 2 show the equivalent evolution with time of the oxide microstructure of NF616. A three-layer structure is also observed with this alloy with the same main phases as in 9CrODS: Fe_3O_4 in the outer layer, a mixture of $FeCr_2O_4$ and Fe_3O_4 in the inner layer, and oxide precipitates within metal grains in the internal oxidation layer. Although similar phases are present in both NF616 and the 9CrODS alloy, the oxide morphology is different. The outer and inner oxide layers of NF616 appear denser than those observed in the 9CrODS alloy, and the interface between the inner and internal oxidation layers is jagged as in the 9CrODS 6-week sample. As observed in other alloys, the advancement of the internal oxidation layer appears to be influenced by the material microstructure [12]. Finally, the thickness of the internal oxidation layer is approximately constant throughout, and no Cr_2O_3 film was observed at the internal oxidation layer-metal interface.

The fluorescence data of Figure 2 show chromium enrichment in the inner layer, but no localized chromium enrichment at interfaces, as in the 9CrODS alloy. Nevertheless, a slight localized chromium enrichment is still observed in the NF616 4-week sample, but this sample was coated with an yttrium layer prior to oxidation. A chromium enrichment localized at the interface between the inner and internal oxidation layers had also been observed for the HCM12A sample that had been coated with an yttrium coating prior to oxidation but not the other ones. This is shown in another article [12]. Additionally, the internal oxidation layer is characterized by an exponential decrease in chromium content to reach that of the metal, rather than a relatively steady chromium content as in the 9CrODS alloy.

From the SEM images we can measure the oxide layer thicknesses for both alloys. Table 2 compares the outer and inner layer thicknesses of NF616 and the 9CrODS alloy. The thicknesses for the 9CrODS alloy are much smaller than that for NF616 even though both alloys have similar chromium content.

Figure 3 shows the diffraction data for the NF616 600ºC 2-week sample as a function of distance from the outer-inner layer interface and 2-theta. This data confirms the phase composition of the oxide layers: the outer layer contains only Fe_3O_4, the inner layer contains a mixture of Fe_3O_4 and $FeCr_2O_4$, and the diffusion layer contains mainly $FeCr_2O_4$ precipitates among metal grains. Very few small peaks associated with Cr_2O_3 are observed in the inner part of the inner layer. In the metal, peaks associated with $Cr_{23}C_6$ carbides are present, in agreement with SEM observations, in which small white particles are observed along the metal lath boundaries. Furthermore, in the metal, two peaks are observed near the location of the ferritic iron (110) peak. This suggests that two types of metal grains are present with slightly different unit cell parameters (2.8664 and 2.8794 Å), corresponding to the ferritic and martensitic lath structure of the base metal [13]. Overall, the main difference between the 9CrODS alloy and NF616 is the much smaller amount of Cr_2O_3 present in NF616, especially at interfaces.

Figure 4 shows the diffraction data for the NF616 4-week sample as a function of distance from the outer-inner layer interface and the diffraction angle 2-theta. The main oxide peaks are the same as in the 2-week sample, but additional peaks are observed. In the outer layer, in exact correspondence with the location of the yttrium layer, unidentified peaks are observed corresponding to neither Y_2O_3 nor $YFeO_3$. In the same way as FeO was observed in the 9CrODS 4-week sample, that phase appears in the NF616 4-week sample. In the same location an additional peak is present but has not yet been indexed. Additionally, slightly more intense peaks associated with Cr_2O_3 are seen in both the inner and internal oxidation layers. Peaks associated with chromium carbide $Cr_{23}C_6$ are also seen in the metal. Finally, the ferritic and martensitic peaks are still observed but not in as uniform a manner as in the 2-week sample.

TABLE 2: Comparison of the oxide layer thicknesses for NF616 and the 9CrODS alloy exposed to 600ºC supercritical water.

Samples	NF616			9CrODS		
	2 weeks	4 weeks	6 weeks	2 weeks	4 weeks	6 weeks
Outer Layer (µm)	31	40	51	20	38	38
Inner Layer (µm)	23	31	42	10	23	24

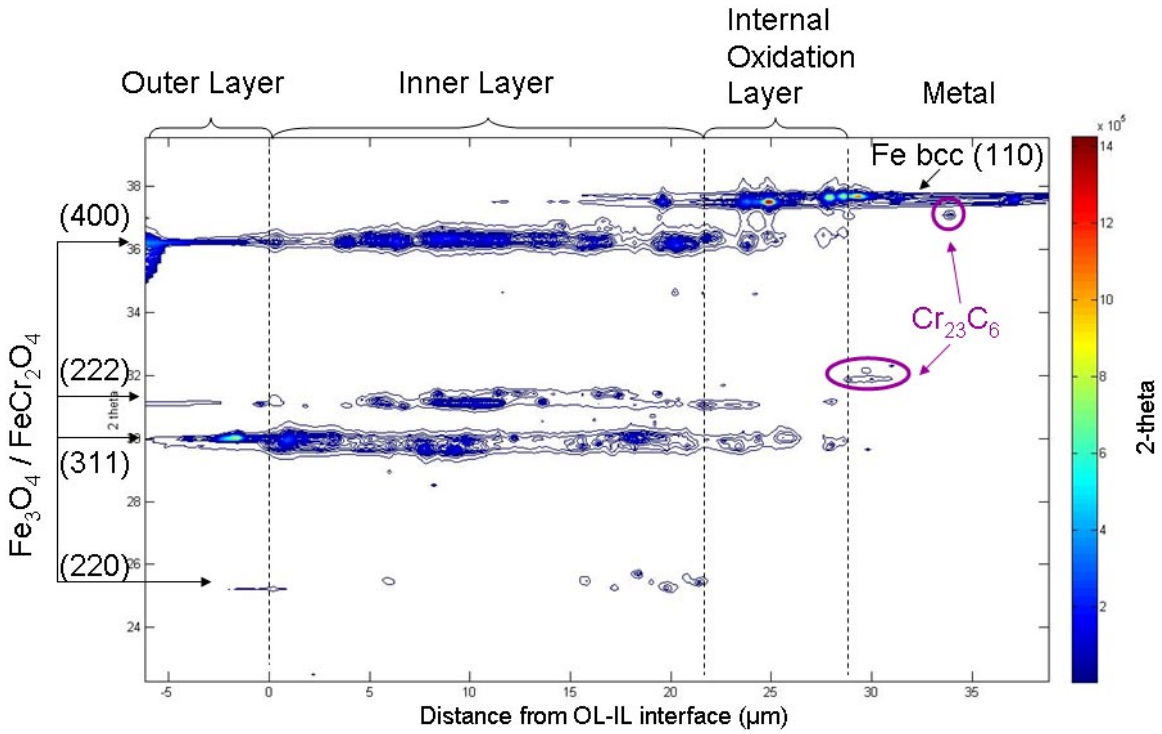

Figure 3: Diffraction data of the NF616 600ºC 2-week sample as a function of distance from the outer-inner layer interface and the diffraction angle 2-theta.

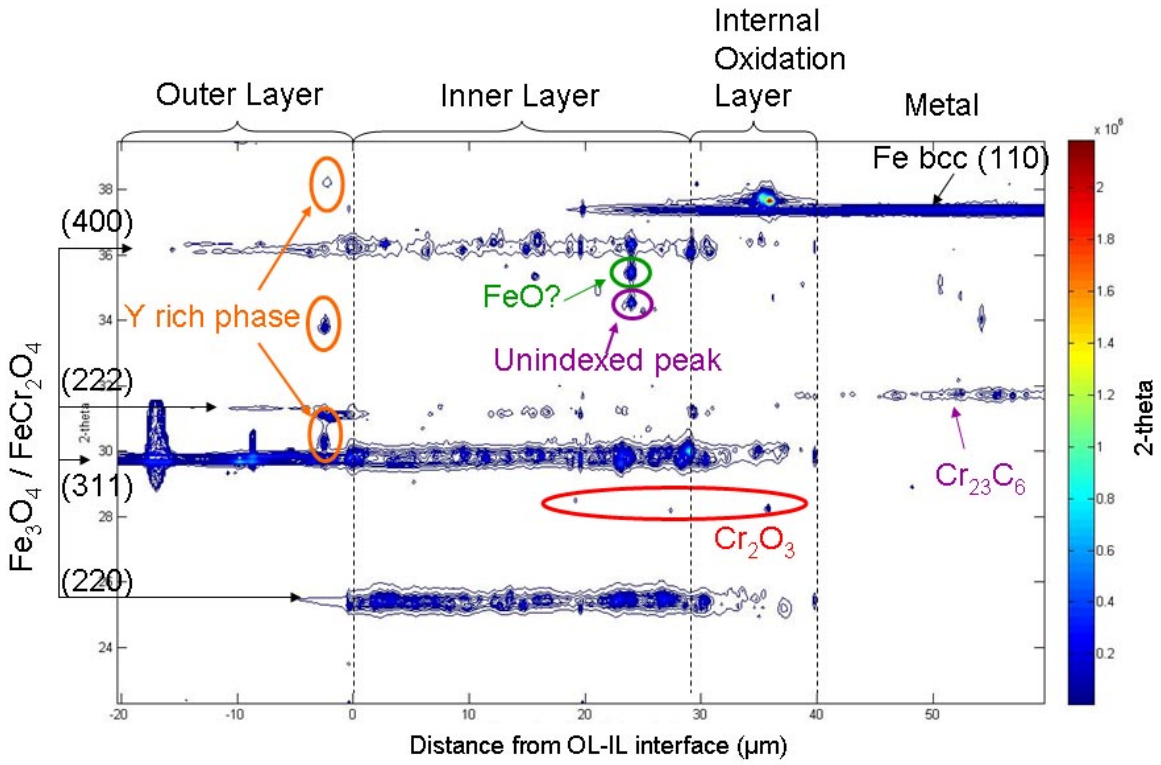

Figure 4: Diffraction data of the NF616 600ºC 4-week sample as a function of distance from the outer-inner layer interface and the diffraction angle 2-theta.

IV. DISCUSSION

The oxide layers formed on both NF616 and the 9CrODS alloys are similar since they have a three-layer structure consisting of an outer layer, an inner layer and an internal oxidation layer. In both cases the oxide phase compositions are the same, showing Fe_3O_4 in the outer layer, a mixture of Fe_3O_4 and $FeCr_2O_4$ in the inner layer, and a mixture of oxide precipitates (mainly $FeCr_2O_4$) and base metal grains in the internal oxidation layer. Only the presence of smaller phases, such as Cr_2O_3, differentiates the oxide microstructure formed on the two alloys.

Figure 5 shows the inner oxide thicknesses for these two alloys as well as for HCM12A when exposed to supercritical water for the times indicated. The inner oxide was chosen because it corresponds to the most protective layer in the oxide. In general oxide protectiveness increases with increasing chromium content [8] (the oxide thickness of HCM12A (11Cr) is smaller than that of NF616 (9Cr)). However 9CrODS has a lower inner oxide thickness than HCM12A, even though its Cr content is lower. This suggests that the presence of the yttrium-rich ODS particles influences the corrosion behavior of the alloy.

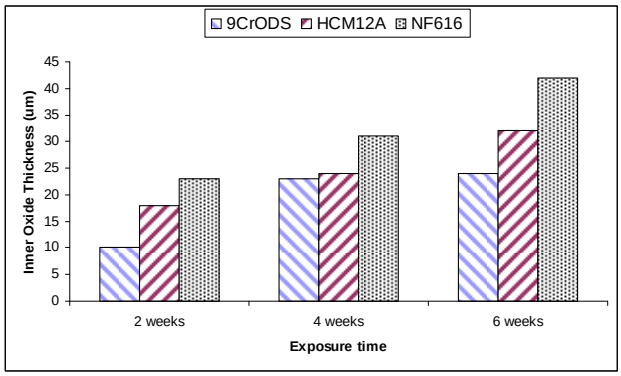

Figure 5: Comparison of the total oxide layer thicknesses for 9CrODS alloy, HCM12A and NF616 exposed in 600ºC supercritical water.

Various researchers have proposed that ODS particles have several corrosion benefits. It has been proposed that they reduce the amount of chromium needed to form Cr_2O_3, thus making it easier to form Cr_2O_3 in alloys containing lower chromium contents than would be necessary to form Cr_2O_3 [4]. Furthermore, it has been proposed that the ODS particles can serve as nucleation sites for the oxide and thus help form Cr_2O_3 [14].The formation of Cr_2O_3 is important for corrosion resistance since it slows down the diffusion of oxygen and iron [15,

[16]. Second, yttrium has been shown to segregate at oxide grain boundaries thus inhibiting oxide grain growth and slowing down diffusion processes [2, 4, 14]. This was also observed for the 9CrODS alloy by Chen et al and was used to explain the enhanced corrosion resistance of that alloy [2].

The main difference between the 9CrODS alloy and NF616 is the lack of Cr_2O_3 in NF616, due to the absence of the ODS particles, which reduce the amount of chromium needed to form Cr_2O_3 to a value closer to 9 wt% (from 20 wt% to about 10-13 wt%) [4]. In the 9CrODS 2 and 4-week samples, Cr_2O_3 was present at the interface between the inner and internal oxidation layers, where a line of large pores was observed [11]. The presence of Cr_2O_3 in this location inhibits the advancement of the oxide in the internal oxidation layer by slowing down the diffusion of oxygen. Additionally, pores form in this location because the iron needed to form the outer layer comes from the inner layer and Cr_2O_3 hinders the replenishment of the pores by inhibiting the outward diffusion of iron from the internal oxidation layer. The absence of Cr_2O_3 at the inner-internal oxidation layer interface may explain the jagged interface and the absence of a line of large pores in NF616. In the same way, the appearance of the Cr_2O_3 film in the 9CrODS alloy between the 2 and 4-week samples seems to have an important influence on the corrosion resistance of the alloy [11].

Additionally, it appears that the presence of yttrium helps segregate chromium at the interface between the inner and internal oxidation layers. The NF616 4-week sample, that was coated with an yttrium layer prior to oxidation, had a slight localized chromium enrichment at that interface, and such an effect of the yttrium coating had also been observed for HCM12A [12]. Consequently, the benefits observed due to the presence of ODS particles in the matrix can partially be obtained by implanting an yttrium layer on the alloy surface prior to oxidation. Nevertheless, the reactive element effect observed with such a technique is nothing compared to the presence of ODS particles.

IV. CONCLUSION

The microstructure of the oxide layers formed on both the 9CrODS alloy and NF616 exposed to 600ºC supercritical water was characterized using microbeam synchrotron radiation diffraction and fluorescence. This analysis was complemented by SEM observations. The main conclusions are:

1. The corrosion of NF616 alloy in 600ºC supercritical water, is faster than that of 9CrODS alloy as illustrated by the larger oxide thicknesses on NF616.
2. The oxide layers formed on both alloys showed a similar three-layer structure with an outer layer of Fe_3O_4, an inner layer containing a mixture of Fe_3O_4 and $FeCr_2O_4$, and an internal oxidation layer containing mainly $FeCr_2O_4$ precipitates mixed among metal grains.
3. Cr_2O_3 was almost absent in the NF616 oxide but was present in large amounts at various interfaces in the 9CrODS alloy. It is suggested that these differences are related to the presence of ODS particles.

ACKNOWLEDGEMENTS

The authors would like to thank Zhonghou Cai and Barry Lai for their help in acquiring the data at the APS facility in Argonne National Laboratory. The authors also thank JAEA for providing the 9CrODS used in this study. This study is a DOE-NERI funded project (DE-FC07-06ID14744) and the use of the APS was supported by the DOE, Basic Energy Sciences, Office of Science under Contract No. W-31-109-Eng-38.

REFERENCES

[1] "A Technology Roadmap for Generation IV Nuclear Energy Systems," U.S. DOE NERAC and Generation IV International Forum GIF-002-00, 2002.

[2] Y. CHEN, K. SRIDHARAN, T. R. ALLEN, and S. UKAI, *Journal of Nuclear Materials*, 359, (2006), 50.

[3] Y. CHEN, K. SRIDHARAN, S. UKAI, and T. R. ALLEN, *Journal of Nuclear Materials*, 371, (2007), 118-128.

[4] J. STRINGER, *Materials Science and Engineering*, A, 120, (1989), 129.

[5] S. OHTUSKA, S. UKAI, M. FUJIWARA, T. KAITO, and T. NARITA, *Materials Transactions*, 46, (2005), 1.

[6] S. UKAI, S. MIZUTA, T. YOSHITAKE, T. OKUDA, M. FUJIWARA, S. HAGI, and T. KOBAYASHIi, *Journal of Nuclear Materials*, 283-287, (2000), 702.

[7] J. BISCHOFF, A. T. MOTTA, and R. J. COMSTOCK, *Journal of Nuclear Materials*, In Press, Accepted Manuscript, (2009).

[8] P. AMPORNRAT and G. S. WAS, *Journal of Nuclear Materials*, 371, (2007), 1-17.

[9] K. SRIDHARAN, S. P. HARRINGTON, A. K. JOHNSON, J. R. LICHT, M. H. ANDERSON, and T. R. ALLEN, *Materials & Design*, 28, (2007), 1177-1185.

[10] K. SRIDHARAN, A. ZILLMER, J. R. LICHT, T. R. ALLEN, M. H. ANDERSON, and L. TAN, "Corrosion Behavior of Candidate Alloys for Supercritical Water Reactors," *Proceedings of*

Proceedings of ICAPP 04, Pittsburgh, PA, (2004).

[11] J. BISCHOFF, A. T. MOTTA, Y. CHEN, and T. R. ALLEN, *Proceedings of NACE Corrosion 2009*, Corrosion in Supercritical Systems, Atlanta, GA, Paper # 09248, (2009).

[12] J. BISCHOFF, A. T. MOTTA, L. TAN, and T. R. ALLEN, *Proceedings of MRS Fall 2008 Conference*, Symposium R: Materials for Future Fusion and Fission Technologies, Boston, MA, Paper # 519941, (2008).

[13] M. JUNG, S.-J. LEE, and Y.-K. LEE, *Metallurgical and Materials Transactions A*, 40, (2009), 551-559.

[14] J. STRINGER, *Oxidation of Metals*, 5, (1972), 11-47.

[15] Y. ISHIKAWA, T. YOSHIMURA, and M. ARAI, Vacuum, 47, (1996), 701-704.

[16] A. C. S. SABIONI, A. M. HUNTZ, F. SILVA, and F. JOMARD, *Materials Science and Engineering A*, 392, (2005), 254-261.